JACS
JOURNAL OF THE AMERICAN CHEMICAL SOCIETY

Communication

pubs.acs.org/JACS

Supramolecular Nanotube of Chaperonin GroEL: Length Control for Cellular Uptake Using Single-Ring GroEL Mutant as End-Capper

Seunghyun Sim,[†] Tatsuya Niwa,[§] Hideki Taguchi,[§] and Takuzo Aida*[,†,‡]

[†]Department of Chemistry and Biotechnology, School of Engineering, The University of Tokyo, 7-3-1 Hongo, Bunkyo-ku, Tokyo 113-8656, Japan

[‡]RIKEN Center for Emergent Matter Science, 2-1 Hirosawa, Wako, Saitama 351-0198, Japan

[§]Research Unit for Cell Biology, Institute of Innovative Research, Tokyo Institute of Technology, Midori-ku, Yokohama 226-8501, Japan

Supporting Information

ABSTRACT: How to modulate supramolecular protein nanotubes without sacrificing their thermodynamic stability? This challenging issue emerged with an enhanced reality since our successful development of a protein nanotube of chaperonin $GroEL_{MC}$ as a novel ATP-responsive 1D nanocarrier because the nanotube length may potentially affect the cellular uptake efficiency. Herein, we report a molecularly engineered protein end-capper (SR_{MC}) that firmly binds to the nanotube termini since the end-capper originates from GroEL. According to the single-ring mutation of GroEL, we obtained a single-ring version of GroEL bearing cysteine mutations ($GroEL_{Cys}$) and modified its 14 apical cysteine residues with merocyanine (MC). Whereas SR_{MC} self-dimerizes upon treatment with Mg^{2+}, we confirmed that SR_{MC} serves as the efficient end-capper for the Mg^{2+}-mediated supramolecular polymerization of $GroEL_{MC}$ and allows for modulating the average nanotube length over a wide range from 320 to 40 nm by increasing the feed molar ratio $SR_{MC}/GroEL_{MC}$ up to 5.4. We also found that the nanotubes shorter than 100 nm are efficiently taken up into HEP3B cells.

One-dimensional (1D) protein assemblies have been found vastly in nature.[1] They execute numerous functions, and the spatiotemporal control of their dimensions is a pivotal issue tightly correlated with their biological functions.[2,3] As a well-known example, actin is a protein fiber that physically supports cells to maintain their structures and enables various intracellular trafficking processes.[1a,2] Such protein nanofibers are designed to be poorly dynamic intrinsically, as they need to maintain their structural integrity under biological conditions. Then, how do they modulate their length? For the length control of actin fibers, protein cofactors such as Tropomodulin and CapZ, which bind firmly to the fiber termini as capping proteins, play an essential role.[3] Even for artificial supramolecular systems, capping reagents have often been used for the length control of 1D fibers.[4] However, no successful examples have been reported for the length control of supramolecular nanotubes including protein nanotubes, without sacrificing their thermodynamic stability.

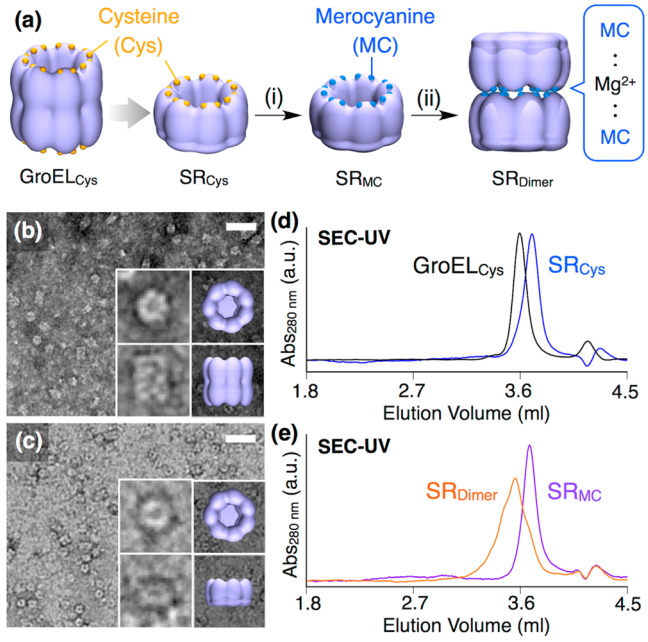

Figure 1. Design and characterization of SR_{MC} as an end-capping protein for the $GroEL_{MC}$-based protein nanotube formed by its Mg^{2+}-mediated supramolecular polymerization. (a) Schematic illustration of the synthesis of SR_{MC} from its precursor SR_{Cys} and Mg^{2+}-mediated self-dimerization of SR_{MC} into SR_{Dimer}. Transmission electron microscopy (TEM) images of reference $GroEL_{Cys}$ (b) and SR_{Cys} (c); scale bar = 50 nm. (d) Size exclusion chromatography (SEC) traces of $GroEL_{Cys}$ (black chart) and SR_{Cys} (blue chart). (e) SEC traces of the merocyanine-attached SR_{Cys} (SR_{MC}, purple chart) and SR_{Dimer} (orange chart) formed upon mixing SR_{MC} with $MgCl_2$ (14 mM).

As described below, we were prompted to tackle a challenging issue to modulate the length of our GroEL-based protein nanotube. A chaperonin protein GroEL is a cylindrical protein assembly that adopts a double-decker structure comprising two identical rings, each of which consists of seven equivalent protein subunits.[5] In 2009, we reported the Mg^{2+}-mediated supramolecular polymerization of a chaperonin $GroEL_{MC}$ having multiple merocyanine units at its apical domains. This

Received: July 31, 2016
Published: August 22, 2016

DOI: 10.1021/jacs.6b07925
J. Am. Chem. Soc. 2016, 138, 11152−11155

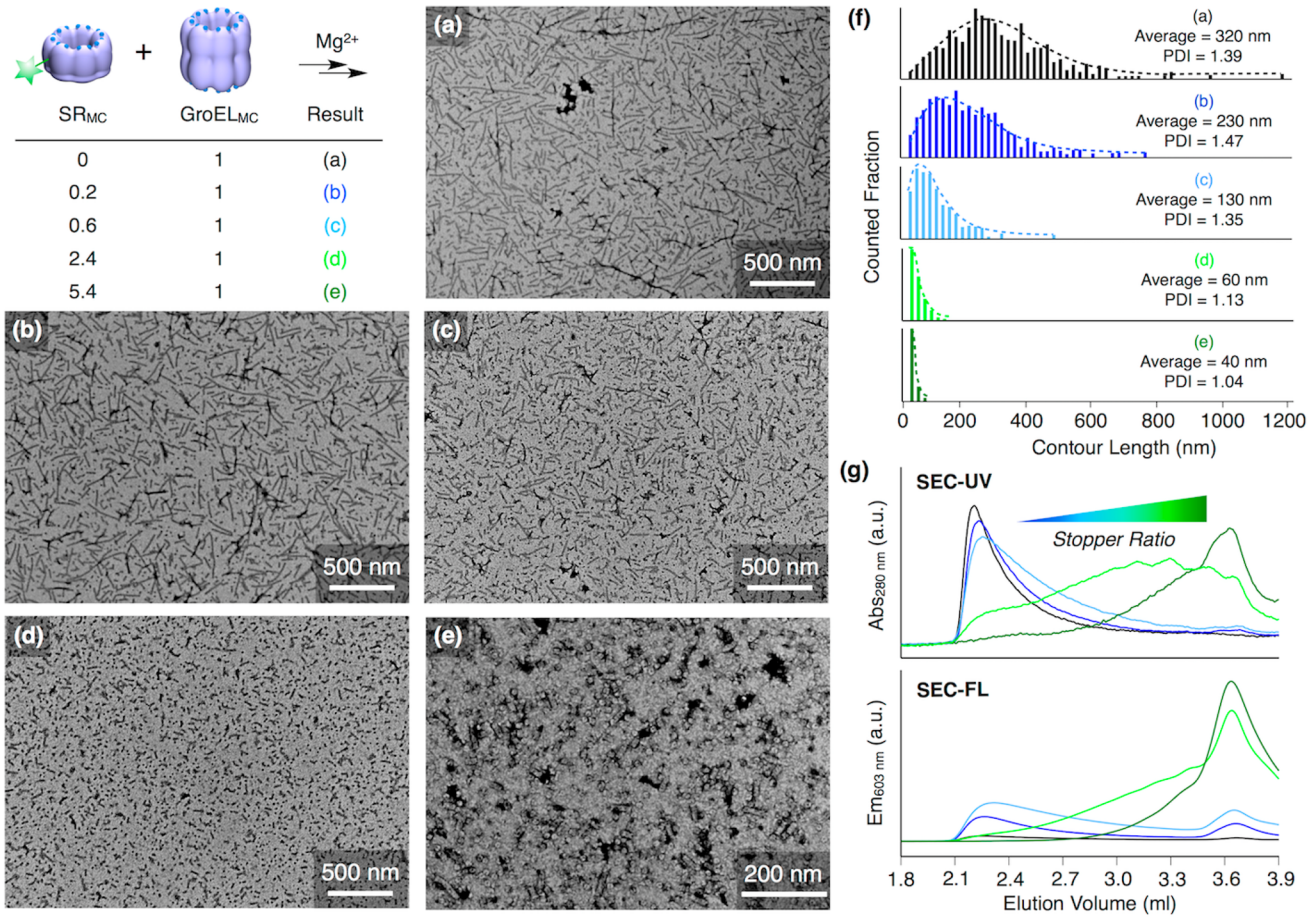

Figure 2. (a–e) TEM images of air-dried $GroEL_{MC}$ nanotube samples stained with uranyl acetate, formed in the supramolecular polymerization of $GroEL_{MC}$ (0.2 μM) with $MgCl_2$ (14 mM) in PBS (10 mM, pH 7.4) in the presence of varying amounts of Alexa Fluor labeled SR_{MC} ($^{AF568}SR_{MC}$). $^{AF568}SR_{MC}/GroEL_{MC}$ = (a) 0, (b) 0.2, (c) 0.6, (d) 2.4, and (e) 5.4. Scale bar = 500 nm (a–d) and 200 nm (e). (f) Histograms of the nanotube length distribution in samples tested, counted from the TEM images (n = 1000). Black bars, sample (a); blue bars, sample (b); sky blue bars, sample (c); light green bars, sample (d); green bars, sample (e). (g) SEC chart monitored by UV (SEC-UV, λ = 280 nm) and fluorescence detectors (SEC-FL, λ_{ex} = 578 nm, λ_{em} = 603 nm) of the Mg^{2+}-mediated polymerization mixtures (a–e).

engineered chaperonin was derived from a GroEL mutant CA-K311C/L314C ($GroEL_{Cys}$) bearing cysteine mutations at the apical domains.[6] In 2013, we found that the supramolecular protein nanotube of $GroEL_{MC}$ serves as an ATP-responsive drug carrier that breaks up into short oligomers in response to intracellular ATP upon cellular uptake because of the mechanical motion of the constituent $GroEL_{MC}$ upon binding with ATP followed by its hydrolysis into ADP.[6b] Not only in intracellular environments but also tumor tissues the ATP concentration is very high; approximately 10^4 times higher than normal tissues.[7] Hence, our GroEL-based protein nanotube may realize cancer-selective drug delivery. Since 1D drug carriers remain still very rare and their internalization behaviors have not been explored,[8,9] we decided to investigate a fundamental issue of how the cellular uptake profile of our $GroEL_{MC}$ nanotube changes with its length. Then, a question arose to us; how can we modulate the length of our protein nanotube without sacrificing its thermodynamic stability? Because our nanotube has a large diameter of 14 nm, we struggled to find an appropriate end-capping agent that could bind strongly to the termini of our protein nanotube.

Meanwhile, we noticed an interesting report by Horwich and co-workers, featuring a single-ring (SR) mutation of GroEL to produce its half-cut version by genetically attenuating the salt-bridges that connect the two rings together in GroEL (Figure 1a). For tailoring a capping protein for our nanotube, we prepared a double genetic mutant (SR_{Cys}) bearing cysteine mutations and the single-ring mutation.[10] Single-ring SR_{Cys} was successfully expressed from *E. coli* bearing genetically engineered plasmid and purified (see the Supplementary Methods and Figure S1). When both of $GroEL_{Cys}$ (Figure 1b, upper inset) and SR_{Cys} (Figure 1c, upper inset) adopt a face-on orientation on a substrate (carbon membrane), transmission electron microscopy (TEM), as expected, does not differentiate between these protein assemblies, because both are supposed to look just like a cyclic heptamer. However, when both adopt an edge-on orientation on the substrate, the TEM imaging readily discriminate between them (Figures 1b,c; lower insets). In size-exclusion chromatography (SEC) using Tris buffer (50 mM, KCl 100 mM, pH 7.4) as an eluent at 25 °C, SR_{Cys} eluted with a larger elution volume than $GroEL_{Cys}$ (Figure 1d). Accordingly, dynamic light scattering (DLS) provided hydrodynamic diameters of 17.5 and 9.5 nm for $GroEL_{Cys}$ and SR_{Cys}, respectively (Figure S2).

To a phosphate buffer solution (PBS) of SR_{Cys} (3.6 μM in PBS 10 mM), merocyanine (MC) was added to covalently modify the 14 apical cysteine thiol groups of SR_{Cys} via a maleimide–thiol Michael reaction (Figure 1a), and the resulting SR_{MC} was passed through a desalting column. As expected, the SEC trace of SR_{MC}

DOI: 10.1021/jacs.6b07925
J. Am. Chem. Soc. 2016, 138, 11152–11155

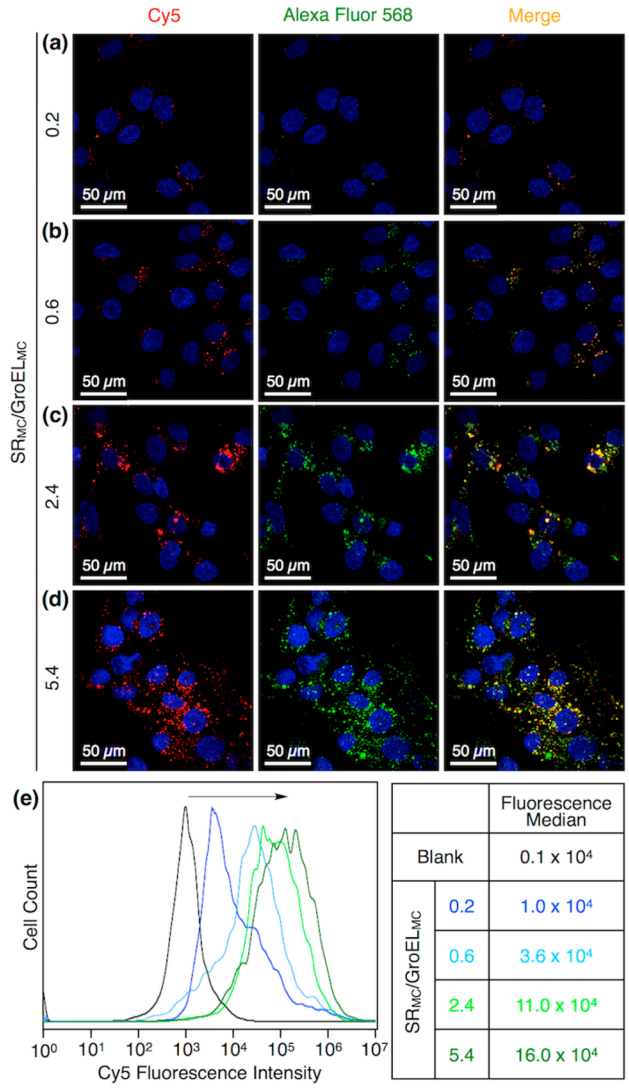

Figure 3. (a–d) Confocal laser scanning microscopy (CLSM) images of HEP3B cells after mixing with fluorescently double-labeled ^{Cy5}GroEL$_{MC}$ nanotubes end-capped with ^{AF568}SR$_{MC}$ having different average lengths. CLSM images visualized based on Cy5 (leftmost), Alexa Fluor 568 (middle), and those after being merged (rightmost) with ^{AF568}SR$_{MC}$/^{Cy5}GroEL$_{MC}$; average nanotube length = (a) 0.2 (230 nm), (b) 0.6 (120 nm), (c) 2.4 (60 nm), and (d) 5.4 (40 nm). Scale bars = 50 μm. (e) Flow cytometry histograms of HEP3B cells based on the Cy5 fluorescence intensities before (blank) and after the treatment of single-labeled nanotubes of ^{Cy5}GroEL$_{MC}$ with varying amounts of SR$_{MC}$.

was virtually identical to that of SR$_{Cys}$ (Figure 1e, purple curve). If SR$_{MC}$ indeed carries MC units at its apical domain, it should self-dimerize upon treatment with Mg^{2+}, in a manner similar to the Mg^{2+}-mediated polymerization of GroEL$_{MC}$. After incubation with $MgCl_2$ (14 mM) for 2 h at 37 °C, the SEC trace of the reaction mixture showed, at the expense of the peak attributed to SR$_{MC}$, the appearance of a new peak assignable to the SR$_{Dimer}$ (Figure 1a) with a similar elution volume to that of GroEL$_{Cys}$ (Figure 1e, orange curve). Subsequent TEM imaging visualized the SR$_{Dimer}$ adopting an edge-on orientation on the substrate (Figure S3). Its diameter was estimated to be approximately 20 nm, which is double the size of SR, accordingly.

The Mg^{2+}-mediated self-dimerization of SR$_{MC}$ indicates its potential as an end-capper for the GroEL$_{MC}$ nanotube. Therefore, we set out to test whether SR$_{MC}$ indeed behaves as expected in the Mg^{2+}-mediated polymerization of GroEL$_{MC}$. For this purpose, SR$_{MC}$ fluorescently labeled with Alexa Fluor 568 (^{FL}SR$_{MC}$) was prepared (see the Supplementary Methods and Figure S4) and its buffer solution (2.2 μM, PBS 10 mM, pH 7.4) was added to that of GroEL$_{MC}$ (2.2 μM, PBS 10 mM, pH 7.4). Then, the GroEL$_{MC}$/^{FL}SR$_{MC}$ mixture was gently stirred and incubated at 37 °C for 1 h to ensure its homogeneity before adding 14 mM of $MgCl_2$ to initiate the polymerization. As shown in Figure 2, the polymerization was conducted at 37 °C for 2 h using a range of mole ratios of SR$_{MC}$/GroEL$_{MC}$ from 0.2 to 5.4. The TEM images in Figures 2a–2e showed that the nanotubes become shorter as the applied mole ratio of SR$_{MC}$/GroEL$_{MC}$ increases. In order to obtain a quantitative insight into the effect of SR$_{MC}$, we counted 1000 nanotubes in individual pictures to yield their histograms (Figure 2f), which displayed a distinct shift of the length distribution from an average value of 320 to 40 nm (for details, see Figure S5). This trend was supported by a marked size reduction, as observed by SEC (Figure 2g, SEC-UV). Here, noteworthy was the fact that the GroEL$_{MC}$ nanotubes formed in the presence of ^{FL}SR$_{MC}$ are fluorescent at 603 nm upon excitation of the Alexa Fluor (578 nm) attached to ^{FL}SR$_{MC}$ (SEC-FL). Furthermore, the higher molecular-weight fraction recorded in SEC-FL was always much less enhanced than that in SEC recorded with a UV detector (SEC-UV). This apparent tendency is reasonable, provided that ^{FL}SR$_{MC}$ attaches only to the nanotube termini. One may also notice in Figure 2g a minor peak assignable to ^{FL}SR$_{Dimer}$ in a low molecular-weight region of the SEC-FL charts (blue and sky blue curves). This implies a slightly higher preference of ^{FL}SR$_{MC}$ for self-dimerization over end-capping (heteromeric connection between SR$_{MC}$ and GroEL$_{MC}$).

Next, we investigated how the cellular uptake efficiency of our GroEL$_{MC}$ nanotube changes with its length. To visualize individual proteins by confocal laser scanning microscopy (CLSM), we labeled GroEL$_{MC}$ with Sulfo-Cy5 (^{Cy5}GroEL$_{MC}$) and SR$_{MC}$ with Alexa Fluor 568 (^{AF568}SR$_{MC}$) (see, the Supplementary Methods and Figure S4) and prepared double-labeled nanotubes with four different average lengths, 230, 120, 60, and 40 nm, by changing the mole ratio of ^{AF568}SR$_{MC}$/^{Cy5}GroEL$_{MC}$ (0.2–5.4) in the presence of a constant amount of ^{Cy5}GroEL$_{MC}$ (2.2 μM, 100 μL). After the polymerization with $MgCl_2$ (14 mM), the reaction mixtures were gently treated with glutaraldehyde (0.25%) for a short period of time (~10 s) to covalently connect the constituent ^{Cy5}GroEL$_{MC}$ units. After desalting and ultracentrifugation, the resulting double-labeled nanotubes were incubated with HEP3B cells (366 nM ^{Cy5}GroEL$_{MC}$, MEM with 10% FBS, 15 h; see the Supplementary Methods for details). As shown by CLSM in Figures 3a–d, the fluorescence signal of ^{AF568}SR$_{MC}$ at the nanotube termini upon dose is mostly overlapped with that of the Cy5 attached to the nanotube main body, implying that SR$_{MC}$ colocalizes with GroEL$_{MC}$ as expected. Notably, CLSM also showed a clear tendency that HEP3B cells fluoresce more as the mole ratio SR$_{MC}$/GroEL$_{MC}$ increases, indicating that shorter nanotubes are internalized more effectively than longer ones. This trend was quantitatively supported by flow cytometry histograms using single-labeled nanotubes prepared with ^{Cy5}GroEL$_{MC}$ and SR$_{MC}$ (Figure 3e). The length-dependent internalization feature of our GroEL$_{MC}$ nanotube is not different from those reported for spherical carriers, most of which have been claimed to be better internalized when they are smaller than 100 nm.[11]

In conclusion, as an end-capper for the Mg^{2+}-mediated supramolecular polymerization of GroEL$_{MC}$, we newly devel-

DOI: 10.1021/jacs.6b07925
J. Am. Chem. Soc. 2016, 138, 11152–11155

oped SR_{MC}, a half-cut $GroEL_{MC}$, by combining together two genetic mutations followed by chemical modification of the apical domain SH groups of the resultant SR_{Cys} by MC. Upon treatment with Mg^{2+}, SR_{MC} underwent self-dimerization, affording a protein cage that may possibly capture guest molecules inside. In addition to this interesting feature, SR_{MC} in the actual polymerization system serves as an efficient end-capper for the $GroEL_{MC}$ nanotube, thereby modulating the average nanotube length over a wide range from 320 to 40 nm. By using HEP3B cells, we found that the cellular uptake efficiency of the nanotube depends critically on its length, where the nanotubes shorter than 100 nm display a much better cellular uptake efficiency than longer ones. We envisage that this unprecedented length-modulable protein nanotube may be applicable to a broad-range of biomedical investigations. Especially, a systematic study on how the nanotube length affects the activity for enhanced retention and permeation (EPR) would be an interesting subject worthy of further investigation.

■ ASSOCIATED CONTENT

Supporting Information

The Supporting Information is available free of charge on the ACS Publications website at DOI: 10.1021/jacs.6b07925.

Details of experimental procedures and micrographs including synthesis of SR_{MC} (PDF)

■ AUTHOR INFORMATION

Corresponding Author

*aida@macro.t.u-tokyo.ac.jp

Notes

The authors declare no competing financial interest.

■ ACKNOWLEDGMENTS

This work was supported by the Japan Society for the Promotion of Science (JSPS) through its Grant-in-Aid for Specially Promoted Research (25000005) on "Physically Perturbed Assembly for Tailoring High-Performance Soft Materials with Controlled Macroscopic Structural Anisotropy". S.S. thanks JSPS for Leading Graduate Schools (MERIT) and Young Scientist Fellowship.

■ REFERENCES

(1) (a) Alberts, B.; Johnson, A.; Lewis, J.; Raff, M.; Roberts, K.; Walter, P. Chapter 16: The Cytoskeleton. In *Molecular Biology of the Cell*; Garland Science: New York, 2002; pp 907. (b) Engler, A. J.; Sen, S.; Sweeney, H. L.; Discher, D. E. *Cell* **2006**, *126*, 677. (c) Herrmann, H.; Aebi, U. *Annu. Rev. Biochem.* **2004**, *73*, 749. (d) Fratzl, P.; Weinkamer, R. *Prog. Mater. Sci.* **2007**, *52*, 1263. (e) Buehler, M. J.; Yung, Y. C. *Nat. Mater.* **2009**, *8*, 175. (f) Xu, K.; Zhong, G.; Zhuang, X. *Science* **2013**, *339*, 452.

(2) (a) Reisler, E. *Curr. Opin. Cell Biol.* **1993**, *5*, 41. (b) Olave, I. A.; Reck-Peterson, S. L.; Crabtree, G. R. *Annu. Rev. Biochem.* **2002**, *71*, 755. (c) Farrants, A. K. *FEBS Lett.* **2008**, *582*, 2041. (d) Zheng, B.; Han, M.; Bernier, M.; Wen, J. K. *FEBS J.* **2009**, *276*, 2669.

(3) (a) Caldwell, J. E.; Heiss, S. G.; Mermall, V.; Cooper, J. A. *Biochemistry* **1989**, *28*, 8506. (b) Weber, A.; Pennise, C. R.; Babcock, G. G.; Fowler, V. M. *J. Cell Biol.* **1994**, *127*, 1627.

(4) (a) De Greef, T. F. A.; Smulders, M. M. J.; Wolffs, M.; Schenning, A. P. H. J.; Sijbesma, R. P.; Meijer, E. W. *Chem. Rev.* **2009**, *109*, 5687. (b) Sijbesma, R. P.; Beijer, F. H.; Brunsveld, L.; Folmer, B. J. B.; Hirschberg, J. H. K. K.; Lange, R. F. M.; Lowe, J. K. L.; Meijer, E. W. *Science* **1997**, *278*, 1601. (c) Furutsu, D.; Satake, A.; Kobuke, Y. *Inorg. Chem.* **2005**, *44*, 4460.

(5) (a) Braig, K.; Otwinowski, Z.; Hegde, R.; Bolsvert, D. C.; Joachimiak, A.; Horwich, A. L.; Sigler, P. B. *Nature* **1994**, *371*, 578. (b) Xu, Z.; Horwich, A. L.; Sigler, P. B. *Nature* **1997**, *388*, 741. (c) Horwich, A. L.; Farr, G. W.; Fenton, W. A. *Chem. Rev.* **2006**, *106*, 1917. (d) Elad, N.; Farr, G. W.; Clare, D. K.; Orlova, E. V.; Horwich, A. L.; Saibil, H. R. *Mol. Cell* **2007**, *26*, 415. (e) Clare, D. K.; Vasishtan, D.; Stagg, S.; Quispe, J.; Farr, G. W.; Topf, M.; Horwich, A. L.; Saibil, H. R. *Cell* **2012**, *149*, 113.

(6) (a) Biswas, S.; Kinbara, K.; Oya, N.; Ishii, N.; Taguchi, H.; Aida, T. *J. Am. Chem. Soc.* **2009**, *131*, 7556. (b) Biswas, S.; Kinbara, K.; Niwa, T.; Taguchi, H.; Ishii, N.; Watanabe, S.; Miyata, K.; Kataoka, K.; Aida, T. *Nat. Chem.* **2013**, *5*, 613. (c) Sendai, T.; Biswas, S.; Aida, T. *J. Am. Chem. Soc.* **2013**, *135*, 11509. (d) Sim, S.; Miyajima, D.; Niwa, T.; Taguchi, H.; Aida, T. *J. Am. Chem. Soc.* **2015**, *137*, 4658.

(7) (a) Pellegatti, P.; Raffaghello, L.; Bianchi, G.; Piccardi, F.; Pistoia, V.; Di Virgilio, F. *PLoS One* **2008**, *3*, e2599. (b) Trabanelli, S.; Očădlíkova, D.; Gulinelli, S.; Curti, A.; Salvestrini, V.; Vieira, R. P.; Idzko, M.; Di Virgilio, F.; Ferrari, D.; Lemoli, R. M. *J. Immunol.* **2012**, *189*, 1303.

(8) (a) Geng, Y.; Dalhaimer, P.; Cai, S.; Tsai, R.; Tewari, M.; Minko, T.; Discher, D. E. *Nat. Nanotechnol.* **2007**, *2*, 249. (b) Nishiyama, N. *Nat. Nanotechnol.* **2007**, *2*, 203. (c) Kolhar, P.; Anselmo, A. C.; Gupta, V.; Pant, K.; Prabhakarpandian, B.; Ruoslahti, E.; Mitragotri, S. *Proc. Natl. Acad. Sci. U. S. A.* **2013**, *110*, 10753.

(9) (a) Bianco, A.; Kostarelos, K.; Prato, M. *Curr. Opin. Chem. Biol.* **2005**, *9*, 674. (b) Gratton, S. E. A.; Ropp, P. A.; Pohlhaus, P. D.; Luft, J. C.; Madden, V. J.; Napier, M. E.; DeSimone, J. M. *Proc. Natl. Acad. Sci. U. S. A.* **2008**, *105*, 11613. (c) Yang, M.; Xu, D.; Jiang, L.; Zhang, L.; Dustin, D.; Lund, R.; Liu, L.; Dong, H. *Chem. Commun.* **2014**, *50*, 4827.

(10) Weissman, J. S.; Hohl, C. M.; Kovalenko, O.; Kashi, Y.; Chen, S.; Braig, K.; Saibil, H. R.; Fenton, W. A.; Horwich, A. L. *Cell* **1995**, *83*, 577.

(11) (a) Jiang, W.; Kim, B. Y. S.; Rutka, J. T.; Chan, W. C. W. *Nat. Nanotechnol.* **2008**, *3*, 145. (b) Zhang, S.; Li, J.; Lykotrafitis, G.; Bao, G.; Suresh, S. *Adv. Mater.* **2009**, *21*, 419. (c) Cabral, H.; Matsumoto, Y.; Mizuno, K.; Chen, Q.; Murakami, M.; Kimura, M.; Terada, Y.; Kano, M. R.; Miyazono, K.; Uesaka, M.; Nishiyama, N.; Kataoka, K. *Nat. Nanotechnol.* **2011**, *6*, 815. (d) Canton, I.; Battaglia, G. *Chem. Soc. Rev.* **2012**, *41*, 2718.

DOI: 10.1021/jacs.6b07925
J. Am. Chem. Soc. 2016, 138, 11152−11155